Plasmonic Detection of Carbohydrate Mediated Biological Events

Isabel García[1,2,*], Jesús Mosquera[1], Javier Plou[1], Luis M. Liz-Marzán[1,2,3,*]

[1]CIC biomaGUNE, Paseo de Miramón 182, 20014 Donostia-San Sebastián, Spain

[2] CIBER de Bioingeniería, Biomateriales y Nanomedicina (CIBER-BBN), Paseo de Miramón 182, 20014 Donostia-San Sebastián, Spain

[3]Ikerbasque, Basque Foundation for Science, 48013 Bilbao, Spain

Abstract:

The incorporation of nanomaterials in glycoscience research has enabled the design of highly selective and sensitive bioanalytical devices for the detection of disease-associated biomarkers. In particular, localized surface plasmon resonance (LSPR) and surface enhanced Raman scattering (SERS) spectroscopies have become powerful biosensing techniques that employ metallic nanostructures to achieve efficient detection of biomolecules. Herein, we review the most recent achievements toward the use of plasmonic nanomaterials together with glycans or glycan-interacting moieties, to detect carbohydrate-mediated biological interactions. The review thus focuses on the use of novel optical nanosensors, mainly LSPR and SERS, for the detection of saccharides, lectins, viruses, bacteria and even whole eukaryotic cells.

Keywords

Plasmonics, Carbohydrates, LSPR sensors, SERS sensors, glycan-mediated interactions.

*Corresponding authors' e-mail: igarcia@cicbiomagune.es; llizmarzan@cicbiomagune.es

Graphical abstract

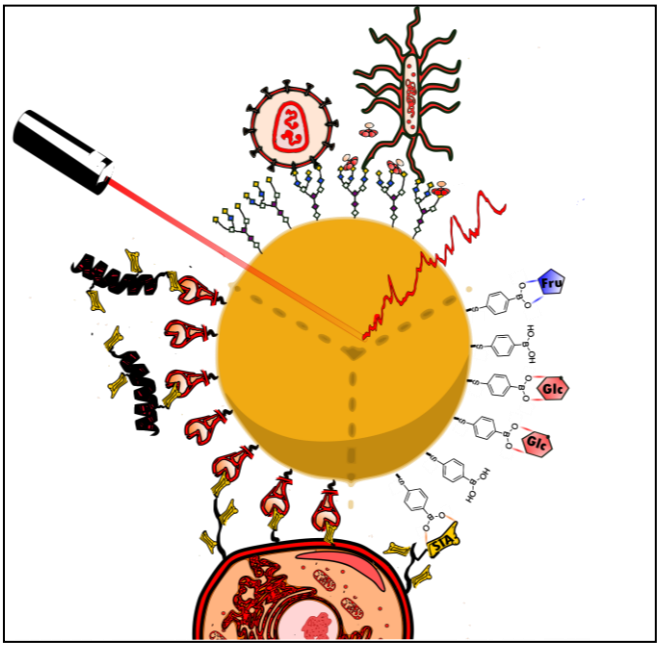

Contents

1. Introduction

Nanotechnology has opened up plenty of opportunities toward the detection of biologically relevant binding events, based on nanoscale sensing elements. Nanomaterials feature a large surface-to-volume ratio and their surface can be readily modified with multivalent ligands to increase their avidity for target molecules. Furthermore, their unique optical properties can be exploited to enhance the performance of traditional assays, facilitating higher sensitivity, even reaching the single molecule detection limit.[1] Of particular interest is the field of plasmonic nanomaterials, which has shown a great potential toward both therapy and diagnostics.[2-7]

Carbohydrates, with lipids, proteins and nucleic acids, are a major class of biologically essential organic molecules that can be found in all living organisms. Carbohydrates are mainly used for energy storage and as metabolic intermediates, but when conjugated to proteins and lipids (yielding glycoproteins, proteoglycans, and glycolipids), they also participate in the regulation of a variety of physiological and pathological processes, such as proliferation and adhesion, immune response, and cell differentiation.[8] The biological roles of carbohydrates as signaling effectors and recognition markers are associated to specific molecular recognition events in which proteins[9] or other carbohydrates[10] are involved. However, individual carbohydrate-based molecular interactions have been shown to be generally weak and, therefore, biomolecules usually present clusters of carbohydrates that interact cooperatively with their natural ligands (multivalent effect), thereby increasing the binding strength.[11] Interestingly, the multivalent carbohydrate presentation can be mimicked by man-made multivalent

systems, which involve multiple synthetic oligosaccharides, [12-17] and have been used to address basic studies, but also as probe molecules and drugs. Mammalian cells are covered by a dense array of carbohydrates known as glycocalix. The glycocalix composition depends on the specific cellular state, and therefore it can provide information about diseases. For example, an increase of α-2,6-sialylation, fucosylation and/or other tumor-associated carbohydrate antigens on the cellular membrane is considered as a biomarker of cancer progression, with diagnostic value.[18-19] In addition, oligosaccharides can be used as disease biomarkers for targeted therapy, and therefore the analysis and characterization of the composition of cellular glycans provide information of relevance to the diagnosis of several diseases.[20] Different strategies can be used to label glycans, including the use of covalent recognizing ligands (e.g. boronic acid), using specific carbohydrate-binding proteins, and via metabolic labeling.

Plasmonics is based on the excitation of surface plasmons, *i.e.* coherent oscillations of electrons excited by an electromagnetic radiation at metal-dielectric interfaces.[21] When the dimensions of plasmonic nanostructures are smaller than the wavelength of the incident light, the interaction between the electromagnetic field and surface charges induces non-propagating oscillations denoted as localized surface plasmon resonances (LSPR).[22] LSPR frequencies in metal nanoparticles depend on their size, shape, organization, inter-particle distance, and dielectric environment, ranging from the visible through the near infrared (NIR).[23,24] A large volume of research has been devoted to the development of reliable methods for the preparation of plasmonic nanostructures with well-defined shape, size and/or interparticle spacing, as basic components of various analytical applications.[25,26] Another important element, the surface chemistry of plasmonic nanomaterials can be finely modulated, so that the metal

surface can be decorated with selected molecules, thereby providing nanomaterials with suitable physicochemical properties to accomplish biosensing.[27-32] Although other materials have been incorporated to improve multifunctionality and sensitivity (e.g. graphene, copper, etc..), Au and Ag nanoparticles (NPs) are the most frequently used components of plasmonic sensors.

Apart from the spectral properties of individual plasmonic NPs, the controlled assembly of plasmonic NPs can lead to additional optical phenomena. When two or more plasmonic nanoparticles are within close proximity, the electromagnetic fields derived from surface plasmons at individual nanoparticles may be affected, resulting in significant changes in the LSPR extinction and scattering spectra.[33] The resulting LSPR coupling-based color changes have been investigated for application in biological assays, using analytes that can induce either assembly or disassembly of NPs.[34]

In addition, the electromagnetic (EM) field concentrated around plasmonic nanostructures can be used for so-called surface-enhanced spectroscopies. The local EM field can influence optical processes such as Raman scattering, such that the signal can be enhanced by many orders of magnitude, resulting in surface-enhanced Raman scattering (SERS) spectroscopy. Plasmon-based SERS sensors show important advantages for biosensing, compared with conventional bioanalytic methods, including high sensitivity with detection limits at picomolar and even zeptomolar levels,[35] resistance to photodegradation, and multiplexing capabilities, while providing intrinsic molecular fingerprint information on biological systems. Plasmonic materials with optimized SERS enhancement have been fabricated through a rational design of nanostructures with controlled morphology and composition,[5,36] to successfully detect different biological entities (e.g. pathogens, cancer cells and biomolecules).[37,38]

We review here recent reports dealing with engineered plasmonic nanostructures, which have been used as signal amplifiers for the optical detection of glycans or glycan-mediated interactions, based on LSPR and/or SERS. More specifically, we highlight the application of plasmonic biosensors to the detection of different biological entities, including saccharides, proteins, bacteria, toxins, viruses and glycans on cellular membranes. We purposely exclude more standard SPR sensors based on commercial chips, typically used to analyze biomolecular interactions.

2. Detection of saccharides

Carbohydrates or saccharides have numerous functions in living organisms, including those related to energy storage and as membrane structural components. In fact, glucose is the sole fuel for the brain of mammals, under normal conditions.[39] The chemistry of saccharides and related molecules is involved in the metabolic pathways of living organisms. Therefore, detecting the concentration of biologically relevant saccharides (e.g. glucose, fructose, galactose) is important in a variety of biological scenarios. An obvious example is monitoring of blood glucose levels, which is of paramount importance because the breakdown of glucose transport has been correlated with diseases such as diabetes, cystic fibrosis, and cancer. In case of diabetes, fluctuations in glucose levels can lead to a wide range of complications, including kidney disease, heart disease, blindness, nerve damage, and gangrene.[40,41]

Unfortunately, despite the importance of saccharides in biology, their detection and quantification is intrinsically challenging due to the lack of endogenous chromophores in their structure. Thus, simple optical techniques such as UV-vis and fluorescence spectroscopies are inefficient. Mass spectrometry analysis is very common for the detection of biomolecules, peptides in particular,[42] but it is also difficult to apply to

underivatized glycans, since these are usually neutral molecules with relatively poor ionization efficiency. The design of selective saccharide sensors is also highly challenging because of their intrinsic chemical structures. Due to the high number of hydroxyl groups in their structure, saccharides have high solvation enthalpies,[43,44] and are also hard to distinguish from an aqueous solvent.[45] As a result, both natural and synthetic receptors tend to show low affinities,[45] e.g. lectin receptors have dissociation constants in the millimolar range for monosaccharides.[46] Recent developments have allowed researchers to overcome the above-mentioned limitations, and achieve saccharide detection. First, it was discovered that boronic acids form a reversible covalent interaction with *cis*-1,2- or 1,3-diols, which are present in basically all saccharides.[47,48] This interaction permits binding of monosaccharides at millimolar concentration and basic pH. Importantly, the hydroxyl group orientation influences affinity, meaning that boronic acids can potentially differentiate saccharides, even if they have similar structures. The binding affinity of phenylboronic acids (PBAs) with monosaccharides follows the order: fructose > galactose > mannose > glucose. It is important to notice that boronic acids interact preferentially with the pair of *syn*-periplanar hydroxyl groups.[49] This kind of hydroxyl arrangement is present in the furanose form of saccharides (5-member ring), which can explain affinity hierarchy in PBAs. In the case of fructose, around 25% of the total concentration of this molecule displays furanose conformation at room temperature. In contrast, the available glucofuranose form in glucose makes up only 0.14% of the total composition under the same conditions. A recent breakthrough in this field has been the application of plasmonic materials for the detection of saccharides, in particular toward SERS-based detection. SERS has been applied to the detection of a wide variety of saccharide derivatives, particularly in combination with boronic acids. Detection of

monosaccharides by SERS is challenging because they feature low Raman cross sections, but also because they adsorb only weakly onto metallic surfaces.[50] In order to solve this problem, Vangala et al. described a straightforward chemical reaction to bind rhodamine-based dyes to carbohydrates, through reductive amination. Since Rhodamine has a high SERS activity, carbohydrates (glucose, lactose, and glucuronic acid) could be detected upon conjugation, with limits of detection (LOD) around 1 nM, using silver nanoparticles as substrates for enhancement.[51]

A common strategy toward increasing the efficiency of SERS detection involves the aggregation of nanoparticle colloids, with so-called plasmonic hot spots being formed at interparticle junctions, whereby SERS enhancement factors can be reached as high as 10^7–10^8, *i.e.* several orders of magnitude higher than those achieved with isolated Au or Ag NPs – usually estimated at 10^2–10^3.[52,53] Xu and coworkers exploited NP aggregation to detect glucose in urine with a LOD of 1 mM.[54] Their system was based on Ag NPs decorated with 4-mercaptophenylboronic acid (4-MPBA), a boronic acid with both a high Raman cross section and a thiol group that ensures strong interaction with Ag. Glucose forms bidentate glucose−boronic complexes with boronic acids,[55] such that one glucose molecule interacts simultaneously with two 4-MPBA molecules through the formation of cyclic boronate, so in the presence of glucose aggregation is induced and hot spots are formed, increasing the SERS signal of 4-MPBA.

As shown above, random aggregation of NPs can be used to enhance SERS signals, however the poor control achieved over the size, geometry, and interparticle distance within these aggregates has a negative impact on reproducibility. In contrast, well-defined plasmonic substrates can also be prepared, typically through deposition on solid supports,[56,57] leading to maximized SERS signals, as well as uniform SERS enhancement factors across the entire surface, owing to their homogenous structure, so

that the reproducibility of SERS analysis is greatly improved.[58] Such solid plasmonic substrates have been proposed for the long-term monitoring of target analytes in real biological systems.[59,60] We present below some examples of supported SERS substrates that have been applied to the detection of monosaccharides.

The first glucose biosensor based on SERS was developed by Van Duyne's group, using "silver film over nanospheres" (Ag-FON) substrates (**Figure 1**), functionalized with a self-assembled monolayer of 1-decanethiol, which served to pre-concentrate glucose within a 0-4 nm thick region where the electromagnetic field is enhanced, so that quantitative glucose detection was achieved over a range of 0 - 250 mM. Importantly, all attempts to detect glucose on silver surfaces, using SERS without a partition layer, were unsuccessful.[50] The Ag-FON design was later improved, using mixtures of thiolated ligands (decanethiol and mercaptohexanol) to obtain a dual hydrophobic/hydrophilic functionality that concentrate glucose closer to the SERS active surface (**Figure 1**B).[61] The practical interest of this system was demonstrated by quantitative glucose measurements *in vivo*. The SERS sensor was subcutaneously implanted in a Sprague-Dawley rat, which allowed the authors to measure the glucose concentration in the interstitial fluid. SERS spectra were acquired using an IR laser (λex = 785nm) and addressing the sensor through an optical window (**Figure 1**). Importantly, the high RMSEP (Root Mean Square Error of Prediction) of this sensor (2.97 mM) is one of their main limitations..[62]

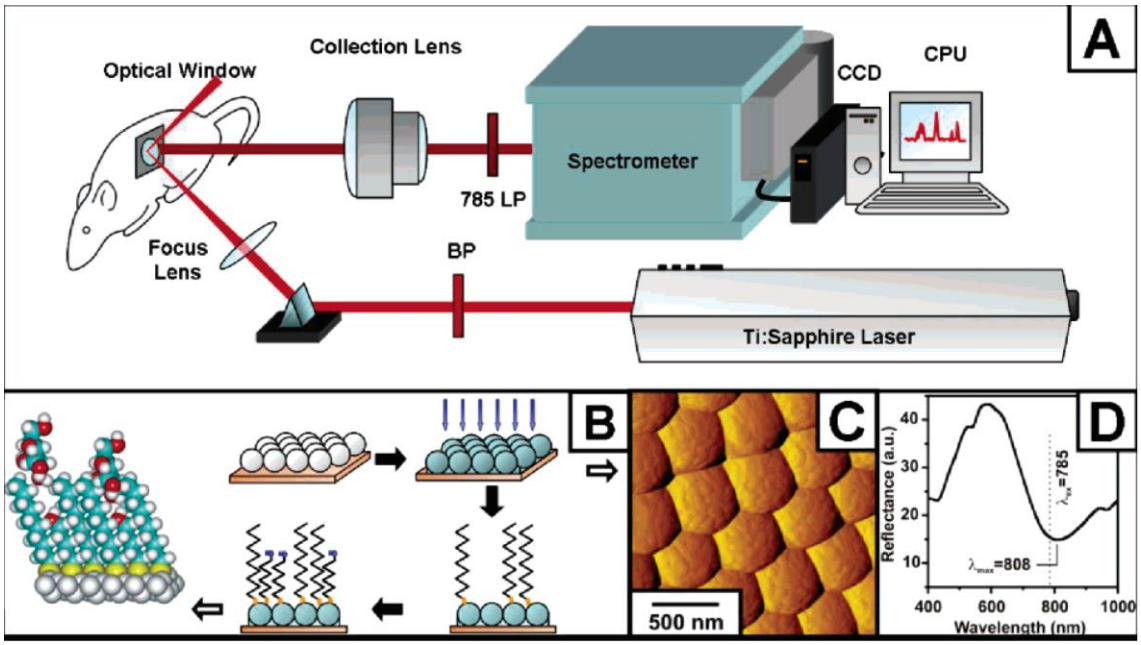

Figure 1. Schematic representation of a glucose SERS sensor *in vivo* based on Ag-FON substrates. (A) Instrumental apparatus. (B) Sensor preparation in which a 200-nm-thick Ag film was deposited onto a nanosphere mask to form Ag-FON surfaces, which were subsequently incubated with decanethiol and mercaptohexanol, to obtain a self-assembled monolayer. (C) Morphology visualized by AFM. (D) Optical characterization of Ag-FON. Reproduced with permission.[62] Copyright 2006, American Chemical Society.

Although the use of self-assembled monolayers has been shown promising for glucose detection, most strategies described to date made use of boronic acids, probably due to their greater simplicity. For example, Bansal and co-workers used 2-thienylboronic acid as a linker to bind glucose molecules to a nanostructured silver film deposited on glass slides. Upon interaction of glucose with the boronic acid, an intense SERS peak was recorded at 983 cm^{-1}, from B-O stretching. This method enabled glucose detection in the range of 1 μM to 500 μM.[63]

An important limitation of standard Raman dyes is that they provide multiple peaks in the fingerprint region (<1800 cm^{-1}), and are thus likely to overlap with the complex peaks derived from endogenous biological species.[64] A solution to this problem may be the use of Raman reporters that exhibit vibrational peaks in the cellular Raman silent

region (between 1800 and 2800 cm^{-1}), in which natural molecules do not present Raman signals. Triosmium carbonyl cluster in combination with boronic acids has been used in a SERS-based assay for glucose detection, using a bimetallic FON as 2D SERS-active substrate (**Figure 2**).[65] Glucose quantification was achieved using a CO stretching vibration of the metal carbonyl at 2111 cm^{-1}, which lies within a silent region of the SERS spectrum. It is worth noting that these assays are based on the tendency of glucose to form bidentate glucose−boronic acid complexes (*vide supra*). It is important to note however, that most of the other physiologically relevant carbohydrates bind to boronic acid as monodentate complexes.[66] Advantage of this property can be taken by using two carbohydrate receptors: a primary 4-MPBA anchored onto a SERS substrate, and a 4-MPBA−triosmium carbonyl cluster conjugate. Glucose is first captured by the primary carbohydrate receptor, then labeled by the second receptor (**Figure 2A**). In this way, it has been possible to selectively detect glucose in the presence of fructose and galactose, with a detection range between 0.1 and 10 mM (**Figure 2B**).

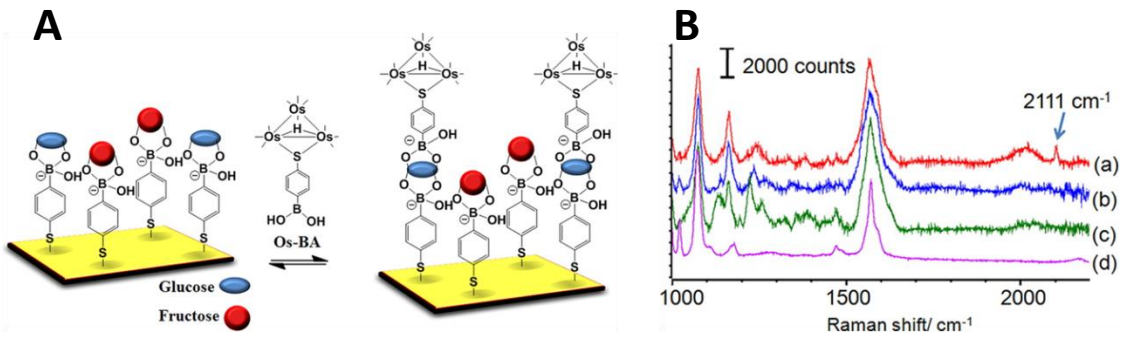

Figure 2. A) Schematic representation of a SERS approach for the detection of glucose using triosmium carbonyl cluster as Raman reporter. B) SERS spectra from a plasmonic substrate incubated with 1 mM of (a) glucose, (b) fructose, (c) galactose, and (d) control, prior to incubation with a triosmium complex. The band at 2111 cm^{-1} was used for quantification. Reproduced with permission.[65] Copyright 2013, American Chemical Society.

An important limitation of the former strategy is that it only operates at pH values around 9, because the interaction between boronic acids and glucose only takes place at basic pH. In order to overcome this limitation, Van Duyne's group, who previously used self-assembled monolayers for SERS detection of glucose, reported a new sensing strategy using bisboronic acid receptors (two units of 4-amino-3-fluorophenylboronic acid).[67] This strategy shares several analogies with the triosmium carbonyl cluster approach. First, both strategies use Au-FON as SERS substrates; second, selective recognition of glucose over other monosaccharides is achieved in both cases taking advantage of the glucose tendency to form bidentate glucose−boronic acid complexes. However, the bisboronic acid receptor enables accurate glucose detection in the 1−10 mM range, at physiological pH. This is a relevant difference that renders this system optimal for *in vivo* glucose detection.

We have seen that the detection based on boronic acids can reach LOD between 1 and 0.1 mM, which is too high for some applications. De la Rosa and co-workers reported the SERS detection of glucose using star-like Au NPs, which is also compatible with neutral pH, and can achieve a detection limit in the nanomolar range.[68] Star-like NPs can provide higher enhancement factors (up to 10^{12}), as compared to spherical NPs (up to 10^{8}), due to the intrinsic hot spots provided by the spike termination.[69] Due to this effect, these particles allow glucose detection at concentrations as low as 10^{-7} M. The authors also showed that additional improvement in the LOD can be achieved by coating the gold nanoparticles with albumin, which can interact with glucose.[70]

Although glucose is the most relevant monosaccharide, other saccharides also feature great biological significance, such as fructose. For example, excessive consumption of fructose is involved in the pathogenesis of diabetic complications, and also plays a role in epidemic development of obesity.[71,72] A SERS-based method has been reported by

Yu and co-workers, to detect fructose in PBS buffer and urine, with a LOD of 0.05 mM under physiological pH conditions. The authors exploited the high affinity between boronic acids and fructose, using a gold quasi-3D plasmonic nanostructure array, coated with a monolayer of 4-MPBA. It is worth highlighting that, as in previous cases, the boronic molecule has a double function as recognition unit and amplifier of SERS signals by the phenyl group.[73]

In summary, several successful strategies to recognize saccharides by plasmonic detection have been described in this section, but the discrimination between carbohydrates differing only in a single chiral center (*i.e.* Glc, Man and Gal) is still a big challenge which needs more research on the design of sugar receptors.

3. Detection of carbohydrate-binding proteins

Lectins are proteins that preferentially recognize carbohydrate structures present on glycolipids and glycoproteins.[74,75] Apart from their well-known cell-agglutinating function, it has been concurrently demonstrated that protein-carbohydrate interactions mediate the selective binding of soluble or membrane-associated lectins to extracellular matrix or cell surface glycans, implicated in various cellular functions (adhesion, migration, differentiation, growth, immunomodulation, host-pathogen interactions).[76,77] Plasmonic glyconanomaterials are thus able to specifically target carbohydrate-binding receptors/proteins; their integration into novel devices (plasmonic sensors) may open new frontiers for detection of tumors, infectious diseases and neurological diseases. In early works, gold- and carbon-based glyconanomaterials were used to study carbohydrate-lectin interactions.[78,79] These pioneering studies demonstrated the feasibility of multivalent glyconanomaterials in protein sensing. Most of the applications of plasmonic nanostructures in biosensing of carbohydrate-binding

proteins are “proofs of principle” based on model lectins (Concanavalin A and others). Table 1 summarizes examples where plasmonic-based glyconanomaterials have been used as optical platforms to detect lectins based in colorimetric assays. In these cases, the interaction between Au NPs decorated with carbohydrates and oligomeric carbohydrate-binding proteins cause the formation of agglomerates. Thus, the short distance between Au NPs enables plasmon coupling, thereby causing red-shift and broadening of the LSPR bands.

Table 1. Colorimetric biosensing of carbohydrate-binding proteins in solution, using gold nanoparticles.

Glycosyl	Detected Protein	Plasmonic NPs	Sensitivity	Reference
α–D-Man	ConA	Au NPs (16 nm)	1 μg/mL	[80]
D-GalNAc	PNA, PSA	Au NPs (1-12 nm)		[81]
β–D-Gal	RCA120	Au NPs (50-150 nm)	100 μg/mL	[82]
Heparan Sulphate	Heparanase	Au NPs (15-16 nm)	0.7–5.6μg/mL	[83]
β–D-Gal/ α–D-Man	RCA120; ConA~~;~~ ~~BSA~~	Au NPs (16 nm)	0.01–0.8 μM (RCA120) 0.7–0.2 μM (ConA)	[84]
Maltose, D-Man, D-Glc, Lac,	ConA	Au NPs (12 nm)	0.03-1 nM	[85]
α–D-Glc, Maltose, maltotriose	ConA, Glucoamylase	Au NPs (12 nm)	1 μM	[86]
α–D-Man	Cyanovirin	Au NPs (22 nm)	100 nM	[87]
D-Man; D-glcNAc, Lac, D-Gal; Sucrose, D-Ara, D-Glc	ConA; GS-II; PNA; SBA	Au NPs (22nm)	10 μg/mL	[88]
Lac, β–CD	PNA; human Gal-3	Au NPs (12 nm)	2 μM	[89]
β–D-Gal	PNA; SNA; SNA; UEA; WGA	Au NPs (10-100 nm)	3.5 nM	[90]
Lac, α–D-Gal; β–D-GlcNAc	RCA120, ConA, WGA	Au NPs (15 nm)	0.5–10 μM (RCA120)	[91]

			300 pM (WGA)	
GlcNAc, Lac	WGA, human Gal-3	Au NPs (14 nm) Au NRs (64 x 16 nm)	0.08 nM (WGA) 0.05 μM (Gal-3)	[92]

Abbreviations: Ara, arabinose; CD, cyclodextrin; Dex, dextran; Fuc, fucose; Gal, galactose; GalNAc, galactosamine, Glc, glucose; GlcNAc, N-acetyl-D-glucosamine; Lac, lactose; Man, mannose; BSA, bovine serum albumin; Gal-3, Galectin-3; ConA, Concanavalin A; GS-II, Griffonia simplicifolia II; PSA, pisum sativum agglutinin; PNA, peanut agglutinin; RCA120, Ricinus communis agglutinin; SBA, soybean agglutinin; SNA, Sambucus nigra agglutinin; UEA, Ulex europaeus agglutinin; WGA, wheat germ agglutinin.

Dark-field microscopy (DFM) is a light scattering-based technique, extensively used to study plasmon resonances in single NPs or NP clusters. The scattering cross section increases with the sixth power of the particle diameter and therefore DFM is used to quantitatively discriminate biologically-driven aggregation. A competitive ELISA-type assay was developed by Tian and collaborators,[93] using a pre-formed supramolecular assembly consisting of mannose-Au NPs and the mannose-binding protein (LCA). This glyco-network can be disassembled in the presence of α–fetoprotein, a biomarker used for the diagnosis of hepatocellular carcinoma. LCA acts as a competitive analyte, interacting with the mannose residues of the as-prepared assembly, and DFM can be used to visualize the biomarker at the single particle level. The authors observed a strong scattering signal produced by the coexistence of Man-Au NP and LCA, whereas upon incubation with cancer serum from patients lower scattering intensity was detected, indicating disaggregation in the presence of the target protein.

Using precisely engineered inter-NP spacers (e.g., polymer grafts), it was possible to control the degree of plasmon coupling between NPs.[94] This principle was demonstrated with poly[(lactose)m-b-(pyridine)$_n$] and bivalent galactose-binding lectin from Ricinus communis (RCA120, Mw = 120 kDa) on gold nanorods (Au NRs). The authors claimed that the developed protein assay yielded a LOD for lectins, down to one picogram per milliliter (fM range) using LSPR-based detection. Interestingly, an unconventional approach was reported for duplexed LSPR sensing of ConA using

patterned Ag NPs.[95] NPs with two different heights (35 and 75 nm) were prepared by nanosphere lithography on a single substrate but spatially separated, with two different LSPR λ_{max} of 683 and 725 nm, respectively. Different Ag NPs were functionalized with mannose and galactose ligands, the chip was exposed to ConA and the LSPRs of the two different regions were monitored over time. High specificity and real time kinetics were obtained from the dual sensor, but high concentration of target proteins (19 μM) was required due to the larger surface of the chip.

On a further development, integration of plasmonic NPs with optical fibers allowed carrying out LSPR sensing in very small volumes. As an example, Suda and co-workers designed a fiber-based sensor incorporating gold nanospheres on the end face of the fiber (**Figure 3**),[96] and maltose and lactose residues were covalently linked to Au NPs for lectin detection. LSPR changes were monitored through reflectance spectra measured by the fiber. This device demonstrated protein sensing with a LOD of 20 nM and the possibility of quantifying carbohydrate-protein interactions using very small measurement volumes. These technological innovations may bring LSPR sensing closer to a practical technology that can be applied in the lab and/or the clinic.

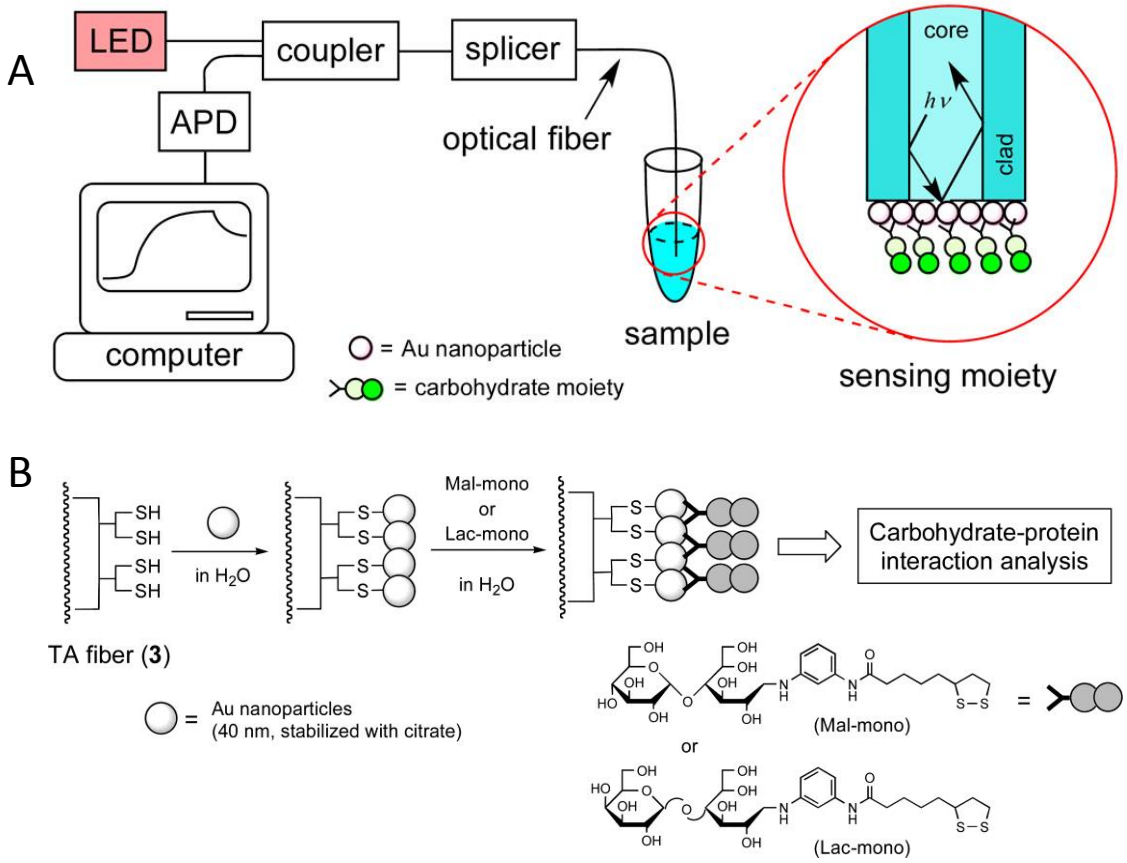

Figure 3. A) LSPR sensor based on an optical fiber derivatized with glycans. B) Immobilization of citrate coated Au NPs onto the fiber end and functionalization with maltose and lactose ligands. Reproduced with permission.[96] Copyright 2017, American Chemical Society.

While the LSPR signal of metal NPs is sensitive to the environmental changes, it provides little information about the nature of interacting molecules. Hence, SERS has been applied as an effective tool to study glycan-protein interactions. A plasmonic substrate based on glycan arrays has been proposed as a label-free detection method to discriminate glycan specificities of Gal-1, Gal 3 and influenza hemagglutinins (HAs).[97] Amino-functionalized glass substrates were used to chemically bind Au NPs (60 nm), and glycans were subsequently immobilized by click chemistry, using glycan derivatives containing azido groups. This label-free detection method yielded minor spectral differences between the normalized SERS spectra of different proteins. Only the use of partial least squares discrimination analysis (PLS-DA) enabled discerning spectra of various classes of carbohydrate-binding proteins, at a low concentration level,

such as 0.1 µg/mL in the case of HA. We can thus see that label-free SERS approaches are available, with promising results for future applications in biology and medicine. However, the interpretation of SERS spectra is often very complex and requires chemometric analysis especially due to low Raman cross sections of the analytes, as well as interferences by many compounds usually present in complex biofluids. These limitations can be overcome by labeling plasmonic nanostructures with Raman-active molecules which provide a strong SERS signal. SERS nanotags have been described to evaluate carbohydrate-protein interactions. Graham's group synthesized SERS active glyconanoparticles to detect a lectin model, ConA, at picomolar levels.[98] Subsequently, Langer et al. expanded their study to discriminate between human tandem type galectins.[99] The authors designed SERS nanotags comprising glycan-decorated Au NPs to monitor in real time the assembly of the nanosensor, upon addition of Gal-9 (**Figure 4A**). Addition of another galectin (Gal-1) or a galactose-binding protein (ECL) did not cause aggregation, as indicated by a negligible SERS signal. By using balanced mixing volume ratios (1:1) for Gal-9 solution and SERS nanotags (**Figure 4B,C**), the aggregation rate could be controlled within a broad working concentration range, between 1.6-to 4 nM of Gal-9 and a LOD of 1.6 nM, even if the LOD was slightly compromised.

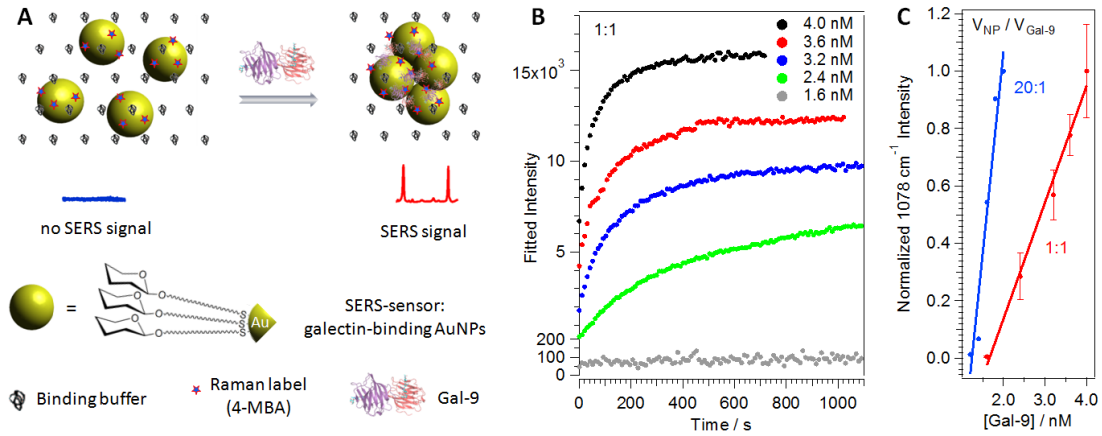

Figure 4. A) SERS nanosensor for detection of Gal-9. B) Time-dependent evolution of the SERS intensity at 1078 cm^{-1} for different Gal-9 concentrations. C) Working concentration range of the sensor in two different configurations of the mixing ratio (Au NPs/ Gal-9). Adapted with permission.[99] Copyright 2017, The Royal Society of Chemistry.

An interesting approach based on molecular imprinting, has recently been demonstrated to provide specific recognition of glycoproteins over other molecules. A gold-based boronate affinity substrate was used for SERS detection of glycoproteins in complex media,[100] in this case to imprint horseradish peroxidase (HRP) and α-fetoprotein (AFP) from human serum on a boronic-acid functionalized plasmonic substrate. A film of molecular imprinted polymers (MIP), generated by self-copolymerization of dopamine and *m*-aminophenylboronic acid (APBA), was formed around the template (the glycoprotein), which was subsequently removed. The captured HRP and AFP proteins were finally labeled with a Raman nanotag (boronate-coated Ag NPs) in a sandwich configuration, for SERS detection. The MIP ensured specificity, whilst SERS detection provided high sensitivity. The prepared sandwich-like complexes generated a larger SERS enhancement, compared to that from the silver-based nanotags. The authors were able to obtain the AFP concentration in serum, from a healthy human with an MIP-bound amount of 13.8 ng/mL. After this original work, the same group extended this methodology to the ultrasensitive and quantitative detection of EPO (Erythropoietin) in human urine.[101] The detection of EPO, a glycoprotein hormone that stimulates red blood cells production, directly in urine or blood, constitutes a mayor challenge in doping analysis due to its short half-life.

A different strategy was used by Lee´s group, based on Förster resonance energy transfer (FRET), to target the lectin Con A.[102] Au NPs were employed as FRET acceptors because of their high extinction coefficient and broad absorption in the visible, which is superimposed onto the emission wavelength of usual FRET donors,

such as quantum dots (QDs). For this purpose, Au NPs were functionalized with thiol-modified mannose to induce the assembly of QDs and Au NPs by hydrogen bonding between the amine groups at QD surfaces and the hydroxyl groups of the mannose on the Au NP surface, thereby leading to strong FRET efficiency. Since Con A presents high affinity to mannose and glucose, when Con A was incorporated to the mixture, the binding between Con A and mannose-stabilized Au NPs attenuated the efficiency of FRET between QDs and Au NPs, leading to recovery of the luminescence.

We thus showed in this section that colorimetric, LSPR and SERS sensors can be applied to the detection of different carbohydrate-binding protein interactions. This field is in rapid progress and is expected to provide information about specific binding partners and eventually to monitor disease states.

4. Sensing of microorganisms

Infections by viruses and bacteria are often mediated by an initial step involving the binding of the pathogen to host receptors. This process is usually regulated by the specific interaction of an envelope protein with glycan receptors at the host surface, thereby generating strong and adhesive forces between them.[103] In this context, the selective interaction between glycans and proteins at the pathogen can be used as an effective means of detecting pathogenic microorganisms. In addition, analyzing the viral/bacterial receptor specificity for a selected glycan is crucial in assessing their potential threat to the public health and tracing viral/bacterial mutations.[104] Hence, interactions between plasmonic glyconanomaterials and pathogens can enable a sensitive and rapid detection method, avoiding time-consuming procedures.

Detection of influenza viruses and their respective envelope protein, hemagglutinin (HA), has become a major focus of interest. Diverse strategies based on glycan-functionalized Au NPs have been developed to provide colorimetric assays that can

determine the interaction between the viral HA protein and host glycan receptors containing terminal sialic acids (SAs). Zhang´s group first devised a simple and efficient method to synthesize SA-stabilized Au NPs, based on a one-pot reaction of $HAuCl_4$, using SA as both reducing and stabilizing agent.[105] In the presence of the influenza B virus, subsequent binding of SA-Au NPs to HA/virus resulted in aggregation of the NPs and a corresponding LSPR shift due to plasmon coupling, leading to a color change. The authors showed a gradual change from red to purple as the amount of viruses in solution was increased. This colorimetric technique was further exploited to discriminate between human and avian influenza virus strains, by virtue of the SA linkage specificity of the corresponding HAs.[106] Au NPs carrying thiolated α-2,6-SA compounds and a thiolated PEG ligand, were prepared by self-assembly on the gold surface. Human viruses bind preferentially to α-2,6 residues, whereas avian influenza viruses bind to α-2,3 residues. Therefore, the synthesized glycan-decorated Au NPs were able to discriminate between human and avian influenza viruses.[106]

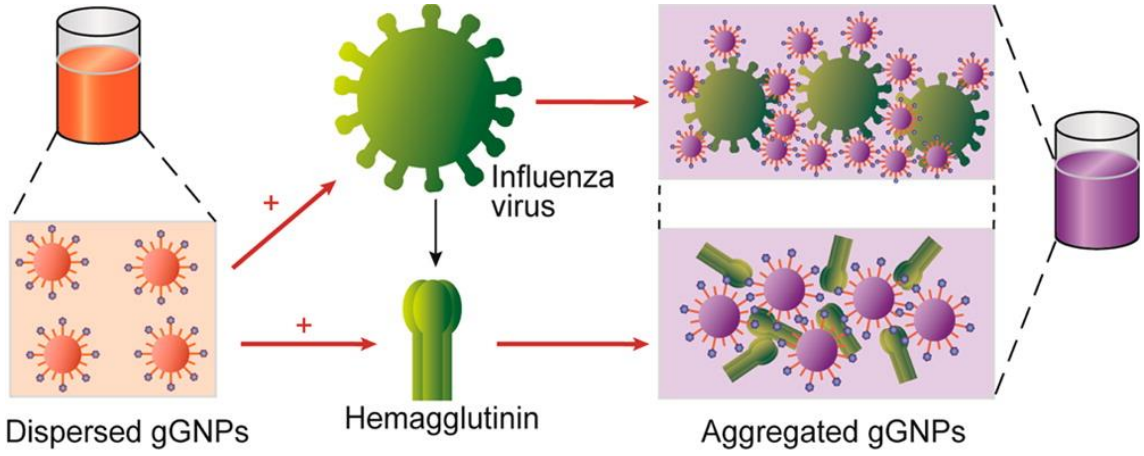

Figure 5. Schematic representation of a colorimetric assay for detection of influenza virus. Glycan-coated Au NPs aggregate when binding to HA or whole virus, leading to a red-to purple color change, which can be quantified by UV-vis spectroscopy, allowing specific detection of viral receptor binding. Reproduced with permission.[107] Copyright 2014, ACS.

Li and colleagues used a chemoenzymatic approach to synthesize two types of glycan decorated Au NPs with either α-2,3 or α-2,6 configuration. A disulfide terminated linker was synthesized by a "click" reaction between alkynes and azide-modified glycans, followed by enzymatic sialylation. Finally, ligand-exchange reactions on citrate-coated Au NPs enabled binding of the glycans onto Au NPs.[107] The authors observed that distinct signal response patterns in colorimetric assays using various glycan-decorated Au NPs provided information about the specificity of the viral receptor (**Figure 5**). This methodology was subsequently used to differentiate influenza virus at the strain, subtype and origin levels, by finely modifying the internal sugars of SA receptors, via e.g. N-acetylation, sulfation, and fucosylation.[108]

Finally, considering the demanding chemoenzymatic synthetic procedure required to prepare sialylated glycan mimics, Fairbanks and co-workers opted to isolate and thiolate sialylglicopeptides from egg yolks, which were then used for the development of a simple and rapid sensor based on sialylated glycans capped Au NPs, for HA and virus detection, with sensitivity down to the nanomolar range.[109]

A broader range of techniques and potential applications based on plasmonic glyconanomaterials can be found within the field of bacteria and toxin sensing. Notwithstanding, the detection of envelope/toxin protein interaction with glycans is still predominating. Gibson and co-workers developed a colorimetric assay to discriminate *E.coli*, based on different expression levels of the FimH adhesin, a mannose/gluco-specific bacterial lectin.[110] Upon binding glyconanoparticles to FimH-positive bacteria, an LSPR shift occurred due to plasmon coupling, enabling the identification of this bacterial strain. In addition, the authors compared the results achieved by direct conjugation of the carbohydrates to the nanoparticles, with those mediated by a poly(ethylene glycol) (PEG) spacer. Higher stability and bio-recognition properties

were observed when a PEG layer was present between the NPs and the carbohydrate, allowing FimH positive bacteria detection, at approximately $1.5x10^7$ colony forming units per mL.

On the other hand, *Vibrio cholera* bacteria are capable of expressing toxins which bind simultaneously to a specific pentasaccharide moiety of a ganglioside (GM1), located on the cellular membrane. Russell and colleagues used a thio-lactose (a disaccharide comprising lactose and a non-reducing terminal galactose) as the simplest molecular recognition element for cholera toxin stabilized onto Au NPs, thereby enabling the development of a colorimetric assay for cholera toxin detection. The assay yielded a LOD of 3 μg mL^{-1}.[111] Graham´s group later sought the detection of cholera toxin, with greater sensitivity than previously achieved. They developed a novel technique (LOD of 56 ng mL^{-1}) based on SERS, which combined Ag NPs mimicking the GM1 surface, with a Raman reporter (RB1). RB1-coated Ag NPs were further functionalized with PEGylated galactose and SA, and cholera toxin samples were subsequently added. Upon aggregation of Ag NPs triggered by Cholera toxin, electromagnetic hot spots were generated, inducing an increase in RB1 SERS signal (**Figure 6**).[112]

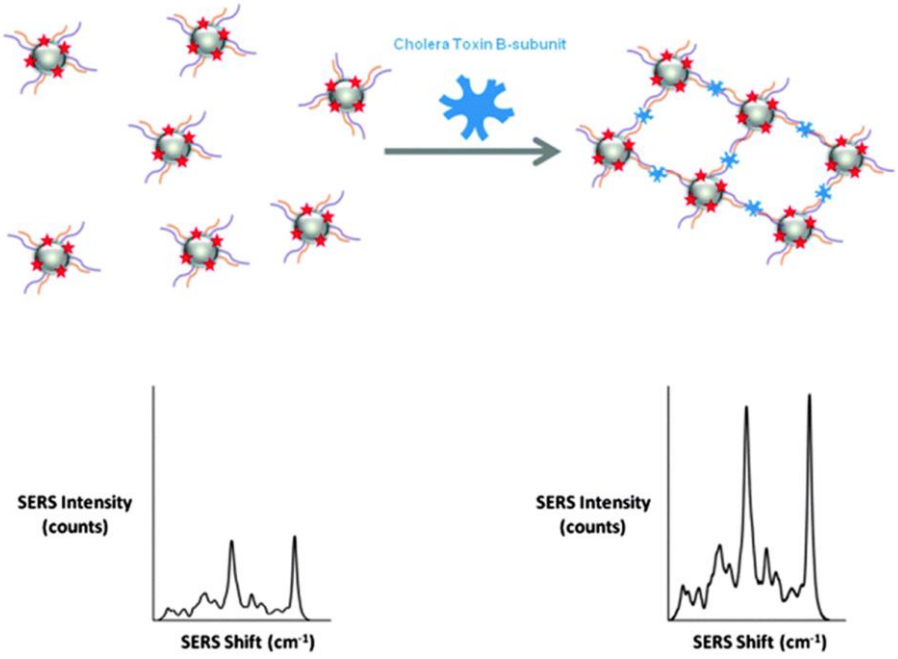

Figure 6. Scheme of a system for detection of cholera toxin, based on changes in the SERS intensity of a Raman reporter, RB1 (red stars), attached to silver nanoparticles (grey). Galactose and SA linkers (orange and purple chains, respectively) enabled silver nanoparticle aggregation, in the presence of cholera toxin and increased SERS signal of the surface bound RB1, upon hot-spot formation. Reproduced under the term of the CC BY 3.0 license.[112] Copyright 2016, The Royal Society of Chemistry.

A method with even higher sensitivity (28 pM) for cholera toxin detection, was accomplished by Lee and coworkers, based on FRET between galactose-stabilized Au NPs and amine-terminated CdTe QDs. In this case, the competitive assay between amino groups of QDs and Cholera toxin toward the selective binding to galactose on Au NPs caused FRET recovery, which was highly dependent on the amount of cholera toxin.[113] Hence, as the amount of cholera toxin increased in the sample, fewer QD-Au NP assemblies were formed, resulting in higher fluorescence intensity.

Overall, smart strategies under development aim to improve the current methods. The results in this section emphasize the potential benefits of integrating plasmonic glyconanomaterials into routine screening of microorganisms, which will enable rapid acquisition of precise information at the strain, subtype and origin levels.

5. Cell phenotyping

The external surface of the cell membrane is covered with glycans that are bound to proteins or lipids, forming the glycocalyx, which is involved in many cell–cell recognition processes such as tumor development, and reflects the developmental stage and the transformation state of a cell. Hence, the glycocalyx can be used to distinguish between healthy cells, diseased cells, or invading organisms. Among the common monosaccharide blocks that constitute the glycocalyx, SAs, a family of 43 negatively charged, 9-carbon monosaccharides, are usually in the terminal position of these glycan

chains. The overexpression of SAs has been shown to correlate with several disease states such as cancer and cardiovascular diseases.[114]

N-Acetylneuraminic (Neu5Ac) acid is the predominant form of SAs and almost the only form found in humans. Jose-Yacaman and coworkers developed a label-free SERS approach for the detection of Neu5Ac. This method comprises a simple competitive adsorption of Neu5Ac over citrate-reduced Ag NPs, allowing the identification of small amounts of aqueous Neu5Ac (10^{-7} M).[115] This approach was later used by Navarro-Contreras to measure Neu5Ac in saliva, for breast cancer diagnosis. The SERS assay was able to correctly identify 94 out of a total of 100 women with breast cancer, and 104 out of a group of 106 healthy women.[116]

Phenylboronic acid (PBA) derivatives have been extensively used for the selective visualization of SA among other glycan constituents of living cells, in combination with plasmonic NPs. This boronic acid forms stable complexes with saccharides, only in its dissociated form, above pH 9 (*vide supra*). Interestingly, PBA specifically binds SAs in its neutral form at physiological pH, with an equilibrium constant of 37, and the same behavior was observed for the thiolated analog 4-MPBA.[117,118] Therefore, PBA has been applied for the selective detection of SAs on the cell surface. The first example of this application was reported by Chen and colleagues, through the demonstration of SERS detection of sialylated glycans, metabolically incorporated with a bioorthogonal Raman reporter on live cells (**Figure 7**). The cell incorporation of SAs bound to Raman reporters was achieved by a metabolic glycan labeling technique, in which cells are fed with monosaccharides containing SERS tags. These synthetic monosaccharides are converted to the corresponding SA-bearing tags, and incorporated as cell surface glycans. Once the synthetic SAs are on the cell surface, they can be detected using Au nanospheres of 120 nm diameter, functionalized with 4-MPBA, which preferentially

binds to SAs, thereby ensuring close proximity between SERS tags and Au NPs. Small organic pendant groups containing alkyne, azide, and nitrile moieties were used as bioorthogonal Raman reporters,[119] which are small enough to be tolerated by the enzymes in the cell, and possess a vibrational mode in the Raman silent region. Previous strategies using similar metabolic incorporation of synthetic saccharides required a second step, where a chemical reporter was covalently conjugated with a fluorescent molecule.[120]

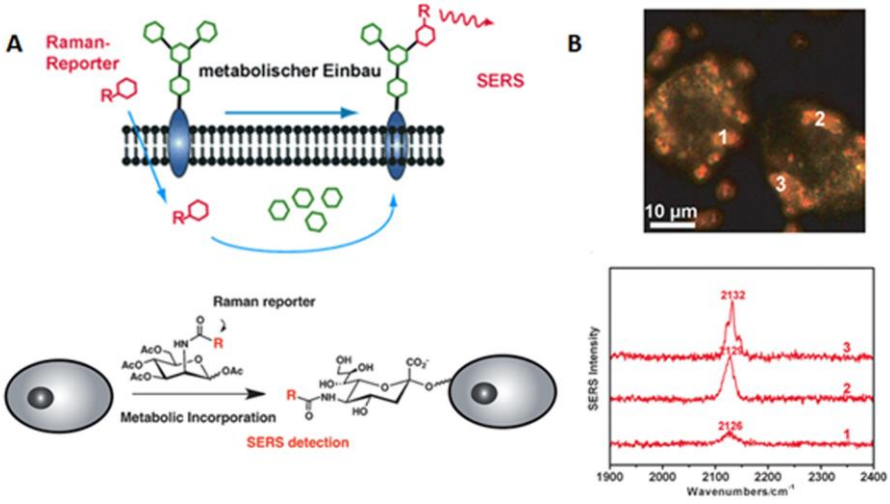

Figure 7. A) The bioorthogonal Raman reporter strategy for SERS detection of sialylated glycans on living cells. B) Dark-field microscopy image of HeLa cells treated with a synthetic mannose containing an azide group, followed by incubation with MPBA-Au NPs and SERS spectra in three different locations of the cell surfaces. Reproduced with permission.[119] Copyright 2011, Wiley-VCH.

Liang and coworkers recently managed to avoid the need for metabolic incorporation of Raman reporters.[121] Their strategy is based on the triple role of 4-MPBA as SERS reporter, sensing reporter, and target receptor, based on the recognition of PBA and SAs. When this nanosensor binds to SAs, the molecular vibrational modes of 4-MPBA change, which can be traced by the ultrasensitive SERS technique. 4-MPBA was used

in combination with 40 nm silver nanospheres, to develop a SERS nanosensor and investigate SAs expression levels and dynamic changes for different cell types, under external stimuli. For this study, BNL.CL2 cells were selected as the normal cell line, whose SA expression is at a physiological level, and HepG2 and Hela cells were chosen as two representative cancer cell lines. As expected, the results indicated that BNL.CL2 has fewer sialoglycans than cancer cells, thus opening the way toward cell identification and discrimination. Furthermore, the authors showed that the same protocol can also be used to monitor changes on SA at the cell membrane, due to the activity of sialidase, an enzyme that can remove SA from glycoconjugates. Following this methodology, Lagugné-Labarthet and coworkers designed a plasmonic platform for glycan sensing.[122] The novelty of this work resides in combining the 4-MPBA strategy with a high control over cell positioning on the plasmonic substrates, which was achieved using nanofabrication methods to pattern fluorocarbon polymer thin films. This technology offered a controlled density of cells on 4-MPBA sensing areas, facilitating accurate statistical studies of SERS signal and enabling authors to locate the glycan-reporter interaction at a defined position.

SERS enhancement upon aggregation of plasmonic NPs and hot-spot formation, was exploited by Xu and coworkers to detect SAs in cells,[123] based on their own glucose sensor, as described above.[54] The authors wisely took advantage of the different recognition properties of 4-MPBA toward SAs and saccharides under different pHs, to obtain Ag NP aggregates. These assemblies were formed by mixing Ag NPs decorated with 4-MPBA, with glucose under alkaline conditions (pH = 9.18), leading to NP aggregation through formation of bidentate glucose−boronic acid complexes (*vide supra*). The assemblies showed a SERS signal for 4-MPBA, 10 times higher than that for the original NPs, due to hot spot formation. The substrates were then used, at neutral

pH, to detect different expression levels of SA on cell surfaces, using the SERS signal of 4-MPBA. The difference in SERS intensity between HepG2 cells (cancer cell model) and BNL.CL (healthy cells) was amplified by 5-7 times when using the aggregates, thus improving cancer cell differentiation.

Although the former example clearly illustrates how the SERS signal can be improved by formation of hot spots, the glucose strategy results in the formation of large assemblies (<300 nm) with no defined structure. A more sophisticated strategy was also reported for the detection of SAs in the glycocalix, using a single-core–multi-satellite system, based on two different Au NPs, a gold nanoflower (AuNF) functionalized with 5,5-dithiobis(2-nitrobenzoic acid) (DTNB) as Raman reporter and 3-MPBA as SA recognition motif, and dendrimer-encapsulated Au NPs co-modified with DTNB and poly(N-acetylneuraminic acid) (PSA) (**Figure 8**). For the detection of SA, cells were first treated with the gold nanoflower that can identify SA through 3-MPBA, then the dendrimer-encapsulated Au NPs were added. These small NPs specifically bound to the nanoflower probe via the interaction of PSA and the free 3-MPBA on the nanoflower surface, so that a single-core–multi-satellite nanostructure was formed, producing a strong enhancement of the SERS signal due to hot spot formation.[114] This plasmonic strategy proved to be suitable to distinguish cancer cells from normal cells due to differences in the concentration of SAs on the cell surface (**Figure 8B**).

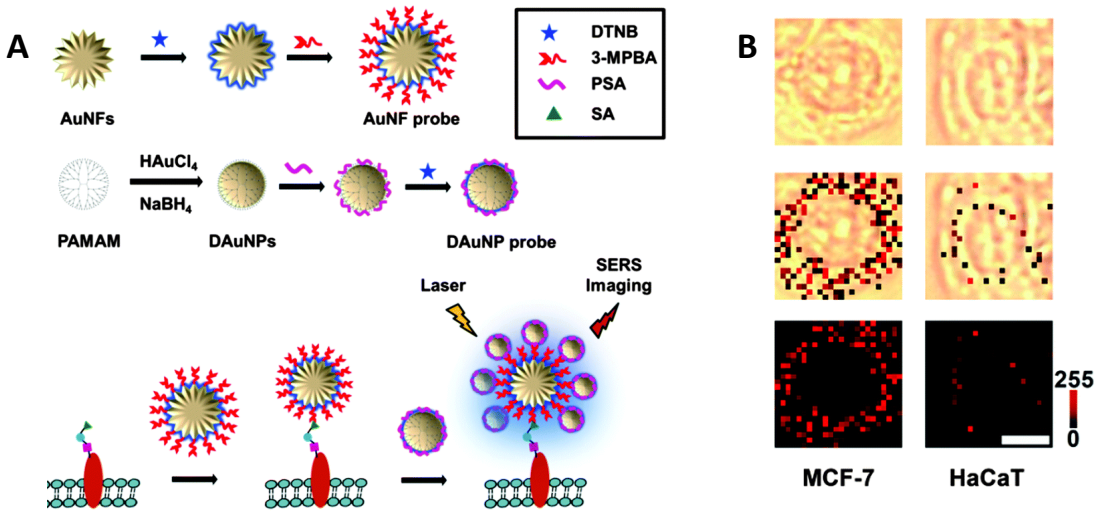

Figure 8. A) Schematic illustration of a strategy to detect SAs in the glycocalix. B) SERS imaging of the cell surface SAs, based on plasmon coupling of the core Au nanoflower with satellite Au NPs. Reproduced with permission.[114] Copyright 2016, The Royal Society of Chemistry.

In order to minimize the background signal typically found in the previous examples, Liu and co-workers developed a new class of Raman reporters comprising alkyne moieties that exhibited a single vibrational peak within the cellular Raman silent region. Such alkyne-bearing Raman reporters were precisely located into the hot spots of dimers made of 30 nm gold nanospheres. The dimers were stabilized using thiolated PEG chains in which an analog of PBA, which enabled the selective recognition of SAs, was covalently bound. This system allowed profiling of SA expression in cancer cells and clinically relevant tissues, with high precision due to the absence of background interference.[124]

We have seen so far the use of boronic acids as a method to study glycocalix composition using plasmonic NPs. However, Graham's group and Huangxian's group reported two different alternatives to the boronic acid method. Graham's strategy was based on using Ag NPs functionalized with lectins. The main advantage of this methodology was that different carbohydrates can be detected, depending on the

selected lectin, in contrast with boronic acids that interact only with SAs at physiological pH. In this research, three different lectin species were used, each displaying a set of carbohydrate specificities. The lectins were bound to the NPs through a heterobifunctional PEG linker, functionalized at one terminus with a benzotriazole forming a strong covalent bond with silver, and was used as SERS reporter. The system was used for discrimination between non-cancerous and cancerous prostate cells.[125] On the other hand, Huangxian's method was based on a metabolic glycan labeling technique, similar to that used by Chen (*vide supra*), which allows decoration of saccharides on the cell surface, using azido moieties. This method enabled protein-specific Raman imaging of glycosylation on the cell surface. The strategy used two different Au NPs: 10 nm and 40 nm. The small NPs carried a Raman reporter and a cyclooctyne-terminated with a PEG linker, and are too small to produce SERS. The larger particles were decorated with aptamers to guide the NPs toward the target protein. The cells were first treated with the small particles, which bound to the SAs through copper-free click chemistry between azide and cyclooctyne. The second particles were then added and bound the target protein through the aptamer. Hence, when the large particles are close to the 10 nm particles containing the SERS reporter, an intense SERS signal was generated (**Figure 9**). This method provides a powerful protocol to uncover glycosylation-related biological processes at a protein-specific level.[126]

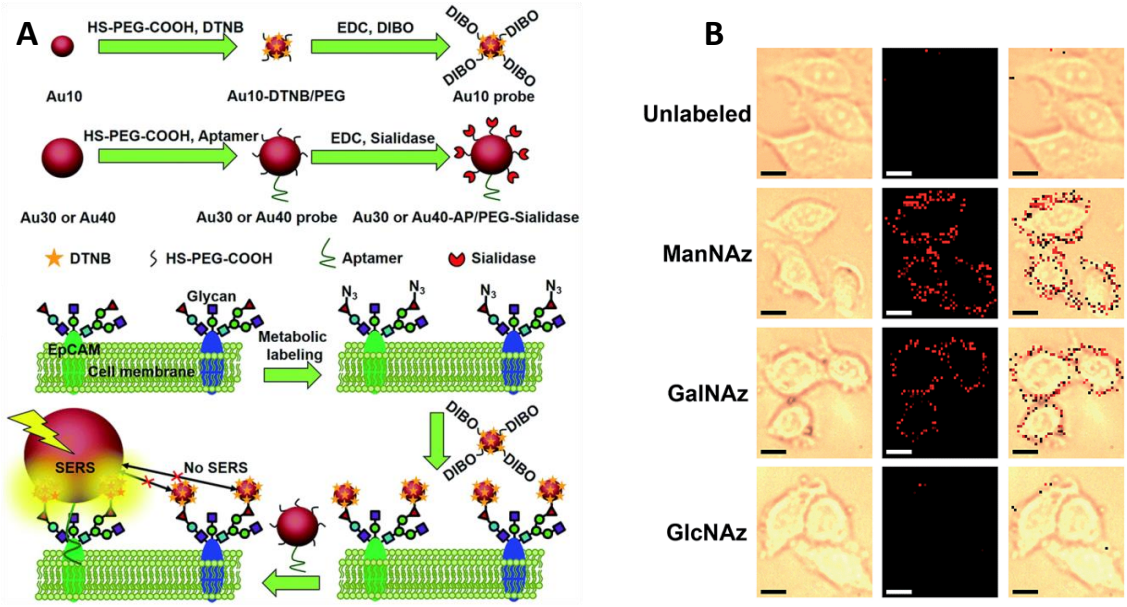

Figure 9. A) Scheme of a strategy to image protein-specific glycans on cell surfaces, using area-specific SERS. B) SERS imaging of different glycans on cells. Reproduced with permission.[126] Copyright 2016, The Royal Society of Chemistry.

A micro-competition system was also developed, for the simultaneous SERS quantification of several glycans on cell surfaces.[127] For this purpose, a system comprising two components was used: SERS-encoded Au NPs functionalized with different lectins to specifically recognize target glycans and glycan-coated Au nanostars assembled onto silica microspheres, which serves as an artificial glycan cellular surface. In this competitive system, glycan expression on the cell surface indirectly determines the amount of SERS-encoded Au NPs bound to the multiple-polysaccharide silica spheres (30 μm) , which can be quickly separated from the mixture and sensitively measured by SERS. As a result of this process, the intensity of Raman signal accurately reflects the amount of glycans on the cell surface and allows for their quantification. Interestingly, this method has been exploited to study the regulation of multiple glycans and opens new opportunities toward *in situ* monitoring of glycans.

By construction of glycan-recognizable probes; glycans and protein specific glycans on cell surfaces can be monitored by SERS imaging using novel labeling strategies. Future developments should focus on the design of targeting tools to achieve time-space analysis of cellular glycans.

6. Conclusions and Outlook

In this review paper, we have highlighted the use of plasmonics-based sensors for the detection of carbohydrates and carbohydrate-mediated interactions. Colorimetric detection methods based on plasmon coupling are well established due to their simplicity. However, these sensors offer relatively low sensitivity and are more vulnerable to interferences, as compared to LSPR and SERS. On the other hand, SERS sensors are quickly expanding, on account of their capability toward chemical analysis, imaging at longer penetration depths and, ultimately, their potential to detect low concentrations such as femtogram/mL or attogram/mL. In the case of LSPR biosensors, much progress is still to be made, to fully exploit their potential as analytical tools for sensing carbohydrate-binding proteins or quantification of microorganisms, such as the characterization of binding kinetics, molecular identification, and detection of conformational changes. The success of future LSPR and SERS sensors will directly depend on the design of new materials and nanostructure architectures, on the improvement of fabrication techniques toward more stable and uniform nanoparticles and, finally, on the incorporation of complementary reporter techniques within the same plasmonic nanostructure. To date, a wide variety of plasmonic sensors have been constructed for the detection of biological interactions involving glycans, but most of them still arise from empirical approaches. The activity toward evaluating glycans on living cell surfaces is still increasing, but it should be noted that most papers deal with fixed cells only. Additionally, only a limited number of assays are available, in which

complex media such as whole blood and human sera are used. Regarding the detection of lectin-glycan interactions, novel and creative strategies are to be expected. Another interesting possibility resides in overcoming the low specificity of lectins by using more selective molecules (e.g. specific carbohydrate-receptors). Finally, the feasibility of discerning between carbohydrates that share the same composition but differ on stereochemistry should also be investigated. The research required to achieve real clinical applications is highly multidisciplinary and demands the involvement of different fields, such as chemistry, physics, biology, mathematics and biomedical engineering.

7. Acknowledgements

The authors acknowledge financial support from the Spanish Ministerio de Economía, Industria y Competitividad (Grant MAT2017-86659-R and Juan de la Cierva fellowship to J.M., FJCI-2015-25080).

8. References

[1] A. B. Taylor, P. Zijlstra, *ACS Sensors* **2017**, *2*, 1103.
[2] A. N. Grigorenko, M. Polini, K. S. Novoselov, *Nat. Photonics* **2012**, *6*, 749.
[3] Y. Wang, B. Yan, L. Chen, *Chem. Rev.* **2013**, *113*, 1391.
[4] S. Zhang, R. Geryak, J. Geldmeier, S. Kim, V. V. Tsukruk, *Chem. Rev.* **2017**, *117*, 12942.
[5] J. Reguera, J. Langer, D. Jiménez de Aberasturi, L. M. Liz-Marzán, *Chem. Soc. Rev.* **2017**, *46*, 3866.
[6] G. A. Sotiriou, *Wiley Interdiscip. Rev. Nanomedicine Nanobiotechnology* **2013**, *5*, 19.
[7] E. Ozbay, *Science.* **2006**, *311*, 189.
[8] M. A. Ferguson, T. Kinoshita, G. W. Hart, *Essentials of Glycobiology. 2nd Edition*, **2009**.
[9] Y. C. Lee, R. T. Lee, *Acc. Chem. Res.* **1995**, *28*, 321.
[10] I. Bucior, M. M. Burger, *Glycoconj. J.* **2004**, *21*, 111.
[11] J. J. Lundquist, E. J. Toone, *Chem. Rev.* **2002**, *102*, 555.
[12] C. Müller, G. Despras, T. K. Lindhorst, *Chem. Soc. Rev.* **2016**, *45*, 3275.
[13] L. L. Kiessling, J. E. Gestwicki, L. E. Strong, *Angew. Chem. Int. Ed.* **2006**, *45*, 2348.
[14] Y. M. Chabre, R. Roy, *Adv. Carbohydr. Chem. Biochem.* **2010**, *63*, 165.

[15] A. Dondoni, A. Marra, *Chem. Rev.* **2010**, *110*, 4949.
[16] N. Yamazaki, S. Kojima, N. V. Bovin, S. André, S. Gabius, H. J. Gabius, *Adv. Drug Deliv. Rev.* **2000**, *43*, 225.
[17] M. Marradi, F. Chiodo, I. García, S. Penadés, *Chem. Soc. Rev.* **2013**, *42*, 4728.
[18] A. Kirwan, M. Utratna, M. E. O'Dwyer, L. Joshi, M. Kilcoyne, *Biomed. Res. Int.* **2015**, *2015*, 1.
[19] D. Feng, A. S. Shaikh, F. Wang, *ACS Chem. Biol.* **2016**, *11*, 850.
[20] L. Krasnova, C.-H. Wong, *Annu. Rev. Biochem.* **2016**, *85*, 599.
[21] W. L. Barnes, A. Dereux, T. W. Ebbesen, *Nature* **2003**, *424*, 824.
[22] S. Link, M. A. El-Sayed, *Int. Rev. Phys. Chem.* **2000**, *19*, 409.
[23] K. L. Kelly, E. Coronado, L. L. Zhao, G. C. Schatz, *J. Phys. Chem. B* **2003**, *107*, 668.
[24] N. Li, P. Zhao, D. Astruc, *Angew. Chem. Int. Ed.* **2014**, *53*, 1756.
[25] L. M. Liz-Marzán, *Langmuir* **2006**, *22*, 32.
[26] S.-W. Hsu, A. L. Rodarte, M. Som, G. Arya, A. R. Tao, *Chem. Rev.* **2018**, 118, 3100.
[27] A. J. Haes, W. P. Hall, L. Chang, W. L. Klein, R. P. Van Duyne, *Nano Lett.* **2004**, *4*, 1029.
[28] W. Ma, H. Kuang, L. Xu, L. Ding, C. Xu, L. Wang, N. A. Kotov, *Nat. Commun.* **2013**, 4, 2689.
[29] S. S. Aćimović, M. A. Ortega, V. Sanz, J. Berthelot, J. L. Garcia-Cordero, J. Renger, S. J. Maerkl, M. P. Kreuzer, R. Quidant, *Nano Lett.* **2014**, *14*, 2636.
[30] M. Singh, M. Holzinger, M. Tabrizian, S. Winters, N. C. Berner, S. Cosnier, G. S. Duesberg, *J. Am. Chem. Soc.* **2015**, *137*, 2800.
[31] J. Yang, M. Palla, F. G. Bosco, T. Rindzevicius, T. S. Alstrøm, M. S. Schmidt, A. Boisen, J. Ju, Q. Lin, *ACS Nano* **2013**, *7*, 5350.
[32] M. Salehi, L. Schneider, P. Ströbel, A. Marx, J. Packeisen, S. Schlücker, *Nanoscale* **2014**, *6*, 2361.
[33] N. J. Halas, S. Lal, W. S. Chang, S. Link, P. Nordlander, *Chem. Rev.* **2011**, *111*, 3913.
[34] M. Sabela, S. Balme, M. Bechelany, J. M. Janot, K. Bisetty, *Adv. Eng. Mater.* **2017**, 19, 1700270.
[35] M. Swierczewska, G. Liu, S. Lee, X. Chen, *Chem. Soc. Rev.* **2012**, *41*, 2641.
[36] S. Schlücker, *Angew. Chem. Int. Ed.* **2014**, *53*, 4756.
[37] D. Cialla-May, X.-S. Zheng, K. Weber, J. Popp, *Chem. Soc. Rev.* **2017**, *46*, 3945.
[38] Z. Wang, S. Zong, L. Wu, D. Zhu, Y. Cui, *Chem. Rev.* **2017**, *117*, 7910.
[39] P. Mergenthaler, U. Lindauer, G. A. Dienel, A. Meisel, *Trends Neurosci.* **2013**, *36*, 587.
[40] P. Luppi, V. Cifarelli, J. Wahren, *Pediatr. Diabetes* **2011**, *12*, 276.
[41] X. Sun, T. D. James, *Chem. Rev.* **2015**, *115*, 8001.
[42] V. H. Wysocki, K. A. Resing, Q. Zhang, G. Cheng, *Methods* **2005**, *35*, 211.
[43] M. Yamashina, M. Akita, T. Hasegawa, S. Hayashi, M. Yoshizawa, *Sci. Adv.* **2017**, *3*, e1701126.
[44] P. Rios, T. S. Carter, T. J. Mooibroek, M. P. Crump, M. Lisbjerg, M. Pittelkow, N. T. Supekar, G. J. Boons, A. P. Davis, *Angew. Chem. Int. Ed.* **2016**, *55*, 3387.
[45] M. Mazik, *Chem. Soc. Rev.* **2009**, *38*, 935.
[46] M. Ambrosi, N. R. Cameron, B. G. Davis, *Org. Biomol. Chem.* **2005**, *3*, 1593.
[47] X. Wu, Z. Li, X.-X. Chen, J. S. Fossey, T. D. James, Y.-B. Jiang, *Chem. Soc. Rev.* **2013**, *42*, 8032.
[48] K. Lacina, P. Skládal, T. D. James, *Chem. Cent. J.* **2014**, *8*, 60.

[49] J. P. Lor, J. O. Edwards, *J. Org. Chem.* **1959**, *24*, 769.
[50] K. E. Shafer-Peltier, C. L. Haynes, M. R. Glucksberg, R. P. Van Duyne, *J. Am. Chem. Soc.* **2003**, *125*, 588.
[51] K. Vangala, M. Yanney, C.-T. Hsiao, W. W. Wu, R.-F. Shen, S. Zou, A. Sygula, D. Zhang, *Anal. Chem.* **2010**, *82*, 10164.
[52] D. Radziuk, H. Moehwald, *Phys. Chem. Chem. Phys.* **2015**, *17*, 21072.
[53] W. E. Doering, S. Nie, *J. Phys. Chem. B* **2002**, *106*, 311.
[54] D. Sun, G. Qi, S. Xu, W. Xu, *RSC Adv.* **2016**, *6*, 53800.
[55] S. Gamsey, A. Miller, M. M. Olmstead, C. M. Beavers, L. C. Hirayama, S. Pradhan, R. A. Wessling, B. Singaram, *J. Am. Chem. Soc.* **2007**, *129*, 1278.
[56] C. Hanske, G. González-Rubio, C. Hamon, P. Formentín, E. Modin, A. Chuvilin, A. Guerrero-Martínez, L. F. Marsal, L. M. Liz-Marzán, *J. Phys. Chem. C* **2017**, *121*, 10899.
[57] T. Udayabhaskararao, T. Altantzis, L. Houben, M. Coronado-Puchau, J. Langer, R. Popovitz-Biro, L. M. Liz-Marzán, L. Vukovic, P. Král, S. Bals, R. Klajn, *Science* **2017**, *358*, 514.
[58] J. J. Giner-Casares, L. M. Liz-Marzán, *Nano Today* **2014**, *9*, 365.
[59] L. Ben Mohammadi, T. Klotzbuecher, S. Sigloch, K. Welzel, M. Göddel, T. R. Pieber, L. Schaupp, *Biosens. Bioelectron.* **2014**, *53*, 99.
[60] G. Rong, S. R. Corrie, H. A. Clark, *ACS Sensors* **2017**, *2*, 327.
[61] O. Lyandres, N. C. Shah, C. R. Yonzon, J. T. Walsh, M. R. Glucksberg, R. P. Van Duyne, *Anal. Chem.* **2005**, *77*, 6134.
[62] D. A. Stuart, J. M. Yuen, N. Shah, O. Lyandres, C. R. Yonzon, M. R. Glucksberg, J. T. Walsh, R. P. Van Duyne, *Anal. Chem.* **2006**, *78*, 7211.
[63] R. Botta, A. Rajanikanth, C. Bansal, Sens. *Bio-Sensing Res.* **2016**, *9*, 13.
[64] Y. Chen, J. Q. Ren, X. G. Zhang, D. Y. Wu, A. G. Shen, J. M. Hu, *Anal. Chem.* **2016**, *88*, 6115.
[65] K. V. Kong, Z. Lam, W. K. O. Lau, W. K. Leong, M. Olivo, *J. Am. Chem. Soc.* **2013**, *135*, 18028.
[66] T. D. James, K. R. A. Samankumara Sandanayake, S. Shinkai, *Angew. Chem. Int. Ed.* **1996**, *35*, 1910.
[67] B. Sharma, P. Bugga, L. R. Madison, A. I. Henry, M. G. Blaber, N. G. Greeneltch, N. Chiang, M. Mrksich, G. C. Schatz, R. P. Van Duyne, *J. Am. Chem. Soc.* **2016**, *138*, 13952.
[68] L. Perez-Mayen, J. Oliva, P. Salas, E. De la Rosa, *Nanoscale* **2016**, *8*, 11862.
[69] L. Rodríguez-Lorenzo, R. A. Álvarez-Puebla, I. Pastoriza-Santos, S. Mazzucco, O. Stéphan, M. Kociak, L. M. Liz-Marzán, F. J. G. De Abajo, *J. Am. Chem. Soc.* **2009**, *131*, 4616.
[70] A. Mohamadi-Nejad, A. A. Moosavi-Movahedi, G. H. Hakimelahi, N. Sheibani, *Int. J. Biochem. Cell Biol.* **2002**, *34*, 1115.
[71] S. E. Lakhan, A. Kirchgessner, *Nutr. J.* **2013**, *12*, 114.
[72] A. I. Cozma, J. L. Sievenpiper, R. J. De Souza, L. Chiavaroli, V. Ha, D. D. Wang, A. Mirrahimi, M. E. Yu, A. J. Carleton, M. Di Buono, A. L. Jenkins, L. A. Leiter, T. M. S. Wolever, J. Beyene, C. W. C. Kendall, D. J. A. Jenkins, *Diabetes Care* **2012**, *35*, 1611.
[73] F. Sun, T. Bai, L. Zhang, S. Liu, A. K. Nowinski, S. Jiang, Q. Yu, *Anal. Chem.* **2014**, *86*, 2387.
[74] R. Mody, S. H. antara. Joshi, W. Chaney, *J. Pharmacol. Toxicol. Methods* **1995**, *33*, 1.
[75] H. Ghazarian, B. Idoni, S. B. Oppenheimer, *Acta Histochem.* **2011**, *113*, 236.

[76] N. Sharon, H. Lis, *Glycobiology* **2004**, *14*, 53R.
[77] N. Sharon, *J. Biol. Chem.* **2007**, *282*, 2753.
[78] H. Kato, A. Yashiro, A. Mizuno, Y. Nishida, K. Kobayashi, H. Shinohara, *Bioorganic Med. Chem. Lett.* **2001**, *11*, 2935.
[79] H. Otsuka, Y. Akiyama, Y. Nagasaki, K. Kataoka, *J. Am. Chem. Soc.* 2001, *123*, 8226.
[80] D. C. Hone, A. H. Haines, D. A. Russell, *Langmuir* **2003**, *19*, 7141.
[81] S. A. Svarovsky, Z. Szekely, J. J. Barchi, *Tetrahedron Asymmetry* **2005**, *16*, 587.
[82] J. M. Bergen, H. A. von Recum, T. T. Goodman, A. P. Massey, S. H. Pun, *Macromol. Biosci.* **2006**, *6*, 506.
[83] Z. Ban, C. J. Bosques, R. Sasisekharan, *Org. Biomol. Chem.* **2008**, *6*, 4290.
[84] C. L. Schofield, B. Mukhopadhyay, S. M. Hardy, M. B. McDonnell, R. A. Field, D. A. Russell, *Analyst* **2008**, *133*, 626.
[85] Y. J. Chuang, X. Zhou, Z. Pan, C. Turchi, *Biochem. Biophys. Res. Commun.* **2009**, *389*, 22.
[86] M. B. Thygesen, J. Sauer, K. J. Jensen, *Chem. Eur. J.* **2009**, *15*, 1649.
[87] X. Wang, O. Ramström, M. Yan, *Anal. Chem.* **2010**, 82, 9082.
[88] H. S. N. Jayawardena, X. Wang, M. Yan, *Anal. Chem.* **2013**, *85*, 10277.
[89] A. Aykaç, M. C. Martos-Maldonado, J. M. Casas-Solvas, I. Quesada-Soriano, F. García-Maroto, L. García-Fuentes, A. Vargas-Berenguel, *Langmuir* **2014**, *30*, 234.
[90] X. Le Hu, H. Y. Jin, X. P. He, T. D. James, G. R. Chen, Y. T. Long, *ACS Appl. Mater. Interfaces* **2015**, *7*, 1874.
[91] L. De Huang, A. K. Adak, C. C. Yu, W. C. Hsiao, H. J. Lin, M. L. Chen, C. C. Lin, *Chem. Eur. J.* **2014**, *21*, 3956.
[92] I. García , A. Sánchez-Iglesias, M. Henriksen-Lacey, M. Grzelczak, L. M. Liz Marzán, S. Penadés, *J. Am. Chem. Soc.* **2015**, *137*, 3686.
[93] X. P. He, X. Le Hu, H. Y. Jin, J. Gan, H. Zhu, J. Li, Y. T. Long, H. Tian, *Anal. Chem.* **2015**, *87*, 9078.
[94] H. Otsuka, Y. Muramatsu, D. Matsukuma, *Chem. Lett.* **2015**, *44*, 102.
[95] C. R. Yonzon, E. Jeoung, S. Zou, G. C. Schatz, M. Mrksich, R. P. Van Duyne, *J. Am. Chem. Soc.* **2004**, *126*, 12669.
[96] M. Wakao, S. Watanabe, Y. Kurahashi, T. Matsuo, M. Takeuchi, T. Ogawa, K. Suzuki, T. Yumino, T. Myogadani, A. Saito, K. I. Muta, M. Kimura, K. Kajikawa, Y. Suda, *Anal. Chem.* **2017**, *89*, 1086.
[97] X. Li, S. J. H. Martin, Z. S. Chinoy, L. Liu, B. Rittgers, R. A. Dluhy, G. J. Boons, *Chem. Eur. J.* **2016**, *22*, 11180.
[98] D. Craig, J. Simpson, K. Faulds, D. Graham, *Chem. Commun*. **2013**, *49*, 30.
[99] J. Langer, I. García, L. M. Liz-Marzán, *Faraday Discuss.* **2017**, *205*, 363.
[100] J. Ye, Y. Chen, Z. Liu, *Angew. Chem. Int. Ed.* **2014**, *53*, 10386.
[101] X. Tu, P. Muhammad, J. Liu, Y. Ma, S. Wang, D. Yin, Z. Liu, *Anal. Chem.* **2016**, *88*, 12363.
[102] K. R. Lim, K.-S. Ahn, W.-Y. Lee, *Anal. Methods* **2013**, *5*, 64.
[103] R. Raman, K. Tharakaraman, V. Sasisekharan, R. Sasisekharan, *Curr. Opin. Struct. Biol.* **2016**, *40*, 153.
[104] O. Ramström, M. Yan, *Chem. Eur. J.* **2015**, *21*, 16310.
[105] C. Lee, M. A. Gaston, A. A. Weiss, P. Zhang, *Biosens. Bioelectron.* **2013**, *42*, 236.
[106] M. J. Marín, A. Rashid, M. Rejzek, S. A. Fairhurst, S. A. Wharton, S. R. Martin,

J. W. McCauley, T. Wileman, R. A. Field, D. A. Russell, *Org. Biomol. Chem.* **2013**, *11*, 7101.
[107] J. Wei, L. Zheng, X. Lv, Y. Bi, W. Chen, W. Zhang, Y. Shi, L. Zhao, X. Sun, F. Wang, S. Cheng, J. Yan, W. Liu, X. Jiang, G. F. Gao, X. Li, *ACS Nano* **2014**, *8*, 4600.
[108] L. Zheng, J. Wei, X. Lv, Y. Bi, P. Wu, Z. Zhang, P. Wang, R. Liu, J. Jiang, H. Cong, J. Liang, W. Chen, H. Cao, W. Liu, G. F. Gao, Y. Du, X. Jiang, X. Li, *Biosens. Bioelectron.* **2017**, *91*, 46.
[109] V. Poonthiyil, P. T. Nagesh, M. Husain, V. B. Golovko, A. J. Fairbanks, *ChemistryOpen* **2015**, *4*, 662.
[110] S.-J. Richards, E. Fullam, G. S. Besra, M. I. Gibson, *J. Mater. Chem. B* **2014**, *2*, 1490.
[111] C. L. Schofield, R. A. Field, D. A. Russell, *Anal. Chem.* **2007**, *79*, 1356.
[112] J. Simpson, D. Craig, K. Faulds, D. Graham, *Nanoscale Horizons* **2016**, *1*, 60.
[113] K. S. Ahn, K. R. Lim, D. Jeong, B. Y. Lee, K. S. Kim, W. Y. Lee, *Microchem. J.* **2016**, *124*, 9.
[114] W. Song, L. Ding, Y. Chen, H. Ju, *Chem. Commun.* **2016**, *52*, 10640.
[115] E. Vinogradova, A. Tlahuice-Flores, J. J. Velazquez-Salazar, E. Larios Rodriguez, M. Jose-Yacaman, *J. Raman Spectrosc.* **2014**, *45*, 730.
[116] A. Hernández-Arteaga, J. de Jesús Zermeño Nava, E. S. Kolosovas-Machuca, J. J. Velázquez-Salazar, E. Vinogradova, M. José-Yacamán, H. R. Navarro Contreras, *Nano Res.* **2017**, *10*, 3662.
[117] H. Otsuka, E. Uchimura, H. Koshino, T. Okano, K. Kataoka, *J. Am. Chem. Soc.* **2003**, *125*, 3493.
[118] K. Djanashvili, L. Frullano, J. A. Peters, *Chem. A Eur. J.* **2005**, *11*, 4010.
[119] L. Lin, X. Tian, S. Hong, P. Dai, Q. You, R. Wang, L. Feng, C. Xie, Z. Q. Tian, X. Chen, *Angew. Chem. Int. Ed.* **2013**, *52*, 7266.
[120] S. T. Laughlin, C. R. Bertozzi, *Proc. Natl. Acad. Sci.* **2009**, *106*, 12.
[121] L. Liang, H. Qu, B. Zhang, J. Zhang, R. Deng, Y. Shen, S. Xu, C. Liang, W. Xu, *Biosens. Bioelectron.* **2017**, *94*, 148.
[122] M. Tabatabaei, G. Q. Wallace, F. A. Caetano, E. R. Gillies, S. S. G. Ferguson, F. Lagugné-Labarthet, *Chem. Sci.* **2016**, *7*, 575.
[123] R. Deng, J. Yue, H. Qu, L. Liang, D. Sun, J. Zhang, C. Liang, W. Xu, S. Xu, *Talanta* **2018**, 179, 200.
[124] H. Di, H. Liu, M. Li, J. Li, D. Liu, *Anal. Chem.* **2017**, *89*, 5874.
[125] D. Craig, S. McAughtrie, J. Simpson, C. McCraw, K. Faulds, D. Graham, *Anal. Chem.* **2014**, *86*, 4775.
[126] Y. Chen, L. Ding, W. Song, M. Yang, H. Ju, *Chem. Sci.* **2016**, *7*, 569.
[127] Y. Chen, L. Ding, J. Xu, W. Song, M. Yang, J. Hu, H. Ju, *Chem. Sci.* **2015**, *6*, 3769.